Unique Structural and Mechanical Properties of Ultrathin Au Films Grown on Dendrimer-Mediated Substrates

Shane C. Street,*,‡ A. Rar,† J. N. Zhou,† W. J. Liu,† and J. A. Barnard*,§

Center for Materials for Information Technology and Departments of Chemistry and Metallurgical and Materials Engineering, The University of Alabama, Tuscaloosa, Alabama 35487-0209

Received September 21, 2000. Revised Manuscript Received January 6, 2001

Evidence is presented here for very significant improvements in film quality when Au is deposited on a self-assembled monolayer of amine-terminated poly(amidoamine) (PAMAM) dendrimers (generation G8) on SiO_x. In addition, the nanomechanical response of the monolayer dendrimer film itself and the Au/dendrimer bilayer configuration is reported for the first time. Ultrathin (12.5 nm) Au grown on the native oxide of Si(100) results in an apparently continuous but poorly adherent film with vertical RMS roughness, ≈1 nm, and occasional, very much larger scale (≈75 nm) features. Dendrimer-mediated Au films have substantially reduced roughness (≈0.4 nm) and no large-scale features. Nanoindentation studies demonstrate surprisingly large differences in the mechanical responses of Au films with and without a dendrimer interlayer. The nanoindentation hardness (a measure of resistance to plastic deformation) of the dendrimer-mediated 12.5-nm Au film is significantly higher than that of the 12.5-nm Au layer alone. This mechanical strengthening is attributed to the compressed and confined nature of the dendrimer interlayer and points to the possibility of using hybrid organic/inorganic nanocomposites as tribomaterials.

Introduction

Dendrimers are three-dimensional, globular, highly branched macromolecules made up of a central core surrounded by repetitive units all enclosed by a terminal group "shell". They can be synthesized with highly controllable sizes (they are essentially monodisperse) determined by the core type, extent of branching, and nature of the end groups, in the range from a few to several tens of nanometers in diameter.[1,2] They have received intensive interest associated with their variable size, the controllable chemistry of their surfaces, and their potential for serving as the host for metal (and other) nanoparticles.[3−5] Dendrimers also readily form monolayers on technologically interesting substrates using simple cleaning, dipping, and rinsing procedures.[6] Dendrimer monolayers are just beginning to receive attention with regard to their adhesive and frictional behavior and related potential applications.[6,7] Direct probes of the nanomechanical response of dendrimer monolayers via nanoindentation have not yet been reported.

Crooks and co-workers recently explored the use of amine-terminated PAMAM dendrimer monolayers as adhesion layers for ≈200-nm Au on SiO_x.[6] They pointed out that organic adhesion layers might be useful replacements for metallic interlayers that may interdiffuse and form intermetallic compounds, adversely affecting physical properties, and that relatively simple solution phase deposition might be preferable to more technically demanding methods for forming the interlayer. It was demonstrated that the amine-terminated dendrimers do provide an adequate adhesion layer, particularly those of higher generation number (larger diameters, more spherical in solution,[8] and more surface end groups). Although individual amine−surface, and amine−metal overlayer, interactions are relatively weak, for higher generation PAMAM dendrimers the number of such interactions per molecule appears to be sufficient to provide effective adhesion.

The deposition of metals onto an organic, homogeneous dendrimer monolayer has obvious parallels with models of metal−polymer interactions. The study of metals vapor deposited onto various modified-end group alkylthiol self-assembled monolayers on Au substrates, for instance, is an active area of research.[9−12] We

* To whom correspondence should be addressed. E-mails: sstreet@bama.ua.edu and jbarnard@mint.ua.edu.
† Center for Materials for Information Technology.
‡ Department of Chemistry.
§ Department of Metallurgical and Materials Engineering.

(1) Tomalia, D. A.; Naylor, A. M.; Goddard, W. A. *Angew. Chem.* **1990**, *102*, 119−157.
(2) Tomalia, D. A. *Adv. Mater.* **1994**, *6*, 529−539.
(3) Zhao, M.; Sun, L.; Crooks, R. M. *J. Am.Chem. Soc.* **1998**, *120*, 4877−4878.
(4) Balogh, L.; Tomalia, D. A. *J. Am. Chem. Soc.* **1998**, *120*, 7355−7356.
(5) Zhao, M.; Crooks, R. M. *Adv. Mater.* **1999**, *11*, 217−220.
(6) Baker, L. A.; Zamborini, F. P.; Sun, L.; Crooks, R. M. *Anal. Chem.* **1999**, *71*, 4403−4406.
(7) Zhang, X.; Wilhelm, M.; Klein, J.; Pfaadt, M.; Meijer, E. W. *Langmuir* **2000**, *16*, 3884−3892.
(8) Topp, A.; Bauer, B. J.; Klimash, J. W.; Spindler, R.; Tomalia, D. A.; Amis, E. J. *Macromolecules* **1999**, *32*, 7226−7231.
(9) Jung, D. R.; Czanderna, A. W.; Herdt, G. C. *Bonding at Metal/Self-assembled Organic Monolayer Interfaces*; Mittal, K. L., Lee, K.-W., Eds.; VSP: Utrecht, 1997; pp 189−221.

10.1021/cm000981e CCC: $20.00
Published on Web 04/28/2001

recently reported spectroscopic chemical analysis of the interaction of Au and Al with an adsorbed amine-terminated dendrimer monolayer on the native oxide of Si(100).[13] X-ray photoelectron spectroscopy clearly indicates that the metal penetrates the organic layer.

In addition to the beneficial effects dendrimer monolayers may have on the adhesion of Au to SiO_x, the intriguing possibility that such organic layers may serve as functional components in hybrid nanocomposite tribomaterials also motivates our work. Much of our group's research focuses on ultrathin tribomaterials relevant to applications in advanced data storage devices (and other systems with strong dimensional constraints) and includes recent work on nanocomposite films and interfaces.[14] This has led to efforts to prepare mechanically robust and strongly adherent protective films using novel methods and materials. An important problem associated with mechanically hard protective overlayers is transmission of load forces to the underlayer/substrate. This can lead to delamination of the layers if their responses are not properly matched or permanent plastic deformation of the ostensibly protected underlayer even if the overlayer experiences complete elastic recovery. An alternative approach to protection could be a system in which a tribomechanically tough overlayer is separated from the underlayer by a mechanically accommodating interlayer adherent at both interfaces. While Au is clearly not mechanically tough, it is nevertheles a useful overlayer for initial studies in which the chemical interaction effects can be expected to be minimized. In this context we have undertaken a study of the nanomechanical response of a self-assembled monolayer of poly(amidoamine) dendrimers (generation G8) grown on oxidized Si(100) wafers and of the same monolayer covered with an ultrathin film of evaporated Au.

The nanomechanical response of Au single crystals studied by both interfacial force microscopy (IFM)[15,16] and nanoindentation[17] has received recent attention primarily in the context of initial yielding behavior. IFM was also used to study polycrystalline Au films with rather large grains (≈500 nm).[18] Very recently, scanning force microscopy has been used to study the nanomodulus and nanohardness of small gold islands ≈50-nm thick and several hundred nanometers in diameter.[19] To our knowledge there are no studies of the response of ultrathin nanocrystalline Au films to nanoindentation.

Materials. The following were used as received: H_2SO_4 (concentrated, Fisher Scientific); H_2O_2 (30%, Fisher Scientific); 2-in. Si(100) wafers (Wafer World, Inc.); pure ethanol (McCormick Distilling Co., Inc.). Nochromix (GODAX Laboratories, Inc.) was added to concentrated H_2SO_4 to make up an oxidizing solution for glass cleaning. Starburst PAMAM dendrimers (generation 8, 1024 terminal amine groups, theoretical molecular weight 233 383 amu) were obtained in a methanolic solution from Dendritech, Inc. Au was evaporated from gold slugs (99.995%, Alfa Aesar).

Substrate Preparation and Film Deposition. As has been noted,[6] substrate preparation and cleanliness are critical in obtaining reproducible results in experiments of this type. All glassware was cleaned in normal detergents, followed by generous rinsing with distilled water. The glassware was then cleaned by Nochromix (oxidizer)/H_2SO_4 solution to remove both organic and inorganic matter and thoroughly rinsed again in deionized water. In general, we followed the method detailed by Crooks and co-workers[6] in preparing dendrimers adsorbed to the Si wafers, except that no attempt was made to remove the native oxide from the wafers, other than the piranha etch (below). Note that UV/ozone cleaning for ≈2 min (UVO−Cleaner Model No. 42, Jelight Co., Inc.) was as good as placing the substrates in freshly prepared piranha solution (3:1 H_2SO_4/30% H_2O_2) for 1 h to remove organic impurities. (**Caution**: piranha solution reacts violently with organic matter. Care should be taken in the use and proper disposal of this oxidizer). Nevertheless, for the purpose of ensuring reproducible SiO_x thicknessses, the piranha cleaning method was used for all films measured by nanoindentation. Ellipsometric measurements indicate that the piranha etch treatment leaves a 2.5-nm-thick SiO_x film on the freshly prepared surface. Clean Si wafers were placed in ground-glass-sealed weigh bottles along with 1 μM ethanolic solutions of the PAMAM dendrimers and allowed to remain at least 3 h (usually overnight) before removal. Upon removal the substrates were copiously rinsed with pure ethanol and dried in a stream of dry N_2.

Au deposition was from one of two chambers, both using resistive heating of W boats to achieve vaporization of the metal. The first is a cryo-pumped system with a base pressure of 1×10^{-8} Torr, holding up to six wafers. The second is a turbo-pumped system with a base pressure of $\approx 5 \times 10^{-8}$ Torr holding one whole (2-in.) wafer. In all cases, the deposition rate was ≈0.4 Å/s monitored in situ by a quartz crystal microbalance. The pressure during deposition was typically $\approx 1 \times 10^{-6}$ Torr. Matched pairs of Au on Si wafer samples, with and without the dendrimer interlayer, were obtained from the same deposition (see Figure 1, c and d).

Characterization. Surface topography was characterized by atomic force microscopy (AFM) in "tapping mode" with a standard tip (Digital Instruments, Inc., model D-3000). A three-parameter roughness analysis was carried out using the height-to-height correlation function, $H(r)$, where r is the separation distance, derived from the AFM images.[20] X-ray photoelectron

(10) Herdt, G. C.; Czanderna, A. W. *J. Vac. Sci. Technol. A* **1999**, *17*, 3415−3418.
(11) Fisher, G. L.; Hooper, A. E.; Opila, R. L.; Allara, D. L.; Winograd, N. *J. Phys. Chem. B* **2000**, *104*, 3267−3273.
(12) Carlo, S. R.; Wagner, A. J.; Fairbrother, D. H. *J. Phys. Chem. B* **2000**, *104*, 6633−6641.
(13) Rar, A.; Zhou, J. N.; Liu, W. J.; Barnard, J. A.; Bennett, A.; Street, S. C. *Appl. Surf. Sci.*, in press.
(14) Ruby, C.; Zhou, J. N.; Du, J.; Street, S. C.; Barnard, J. *Surf. Interface Anal.* **2000**, *29*, 38−45.
(15) Kiely, J. D.; Jarausch, K. F.; Houston, J. E.; Russell, P. E. *J. Mater. Res.* **1999**, *14*, 2219−2227.
(16) Kiely, J. D.; Hwang, R. Q.; Houston, J. E. *Phys. Rev. Lett.* **1998**, *81*, 4424−4427.
(17) Corcoran, S. G.; Colton, R. J.; Lilleoddon, E. T.; Gerberich, W. W. *Phys. Rev. B* **1997**, *55*, R16057−R16060.
(18) Tangyunyong, P.; Thomas, R. C.; Houston, J. E.; Michalske, T. A.; Crooks, R. M.; Howard, A. J. *J. Adhesion Sci. Technol.* **1994**, *8*, 897−912.
(19) Kracke, B.; Damaschke, B. *Appl. Phys. Lett.* **2000**, *77*, 361−363.
(20) Li, M.; Wang, G.-C.; Min, H.-G. *J. Appl. Phys.* **1998**, *83*, 5313−5320.

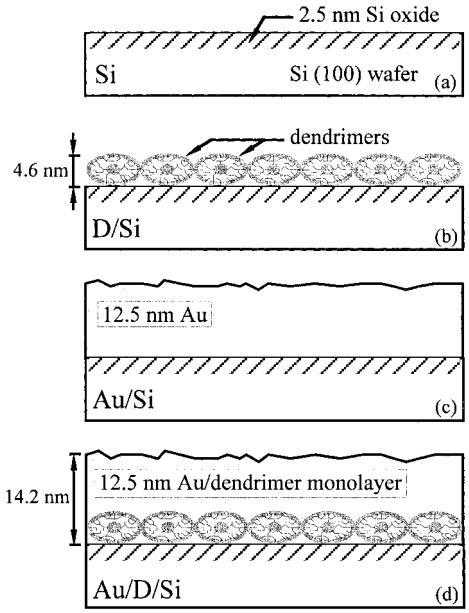

Figure 1. Sample configuration schematics. (a) Si: Si(100) substrate with 2.5-nm-thick SiO_x surface; (b) D/Si: G8 dendrimer monolayer (D) adsorbed on Si; (c) Au/Si: 12.5-nm-thick evaporated Au film on Si; (d) Au/D/Si: 12.5-nm Au evaporated on top of D/Si.

spectroscopy (XPS) measurements were made using a Kratos Analytical Axis 165 system. The spectra were recorded in the FAT mode (80-eV pass energy) using a monochromatic Al *K*α source (1486.6 eV) and normal takeoff angle. Survey spectra were recorded at 1 eV/step and narrow band spectra at 0.1 eV/step. X-ray reflectivity (XRR) measurements in the specular reflectivity mode were performed on a Philips X'pert diffractometer. The data were collected utilizing Cu *K*α radiation (45 kV and 40 mA). A Göbel mirror was used to achieve an intense, parallel X-ray incident beam. The scanning range (2θ) was typically 0.3°−5°. The reflected intensity is measured as a function of incident angle θ and plotted as a function of the scattering vector

$$q = 4\pi \sin \theta/\lambda \qquad (1)$$

where λ is the incident wavelength. The XRR curves were simulated by Philip's proprietary Win-Gixa software (A. J. G. Leenaers and D. K. G. de Boer). Conventional symmetric and asymmetric $\theta-2\theta$ X-ray diffraction (XRD) was also carried out on the same Philips instrument.

Nanomechanical properties were measured by nanoindentation using a Hysitron Triboscope Nanomechanical Testing System with a Berkovich geometry diamond indentation tip. In this system a three-plate transducer is used as an electrostatic actuator and also a capacitive displacement sensor. The transducer is designed to work in conjunction with a commercial AFM and is capable of performing force−displacement measurements with sub-nanometer depth resolution. The shape of the indenter tip was calibrated with a fused silica standard sample. In depth sensing nanoindentation, film hardness, and modulus are calculated from the maximum force and displacement, the slope of the unloading curve, and the calibrated tip area function. The values of these parameters can be obtained directly from the force−displacement curve. The calculation is based on the method developed by Oliver and Pharr.[21]

Results and Discussion

The schematics in Figure 1 illustrate the primary sample configurations used in this study. Figure 1a illustrates the Si(100) substrates used in all experiments. The 2.5-nm-thick SiO_x layer present at the surface of the wafers is noted explicitly here and indicated by crosshatching. At monolayer coverage, the dendrimers are thought to be highly compressed and flattened (Figure 1b). A 12.5-nm-thick Au film was grown on top of the freshly prepared Si substrates by evaporation (Figure 1c). Simultaneously, Au was evaporated on top of the just-described dendrimer monolayer (Figure 1d). For convenience in a subsequent discussion the samples illustrated in Figure 1a−d are referred to as Si, D/Si, Au/Si, and Au/D/Si, respectively, where "D" stands for the G8 dendrimer monolayer. Note that Si in all cases represents the Si wafer with its native oxide as described above.

Surface Topography. AFM images (1 × 1 μm; 10-nm vertical scale) of samples Au/Si and Au/D/Si appear in Figure 2a,b. Clear differences in the surface morphology of the films are evident at this scale. Both Au films are apparently continuous in that the surfaces are gold in color in reflection under an optical microscope and conductive on the macroscopic scale. AFM images of the Au/Si (Figure 2a) sample show occasional ($\approx 1/\mu m^2$) large-scale features (presumably Au clusters) absent in the Au/D/Si images. These features are on average ≈75-nm high (z axis) and ≈80 nm in radius in the plane of the surface, and are roughly hemispherical in shape. After the volumes of the clusters are accounted for, including the effect of a finite AFM tip radius of 10 nm with the assumption that the tip shape is hemispherical, it is clear that the "flat" regions of Au are still ≈11.5-nm thick. The total volume of Au taken up by the clusters is not more than 9% of the total Au slab volume. The observed clustering is the result of the tendency of Au to prefer to interact with itself rather than "wet" the native SiO_x at the surface of the wafer. Indeed, the poor adhesion of the Au to the silica is apparent under an optical microscope, which shows that even the slightest handling of the Au/Si sample can disturb portions of the Au layer. All data for Au/Si samples were obtained from undisturbed regions. A very small Si 2p signal (≈2% atomic concentration, data not shown) is observed in XPS analysis of the Au/Si configuration. This is inconsistent with a perfectly continuous Au layer >10-nm thick and points to the presence of a small area fraction of bare SiO_x resulting from pinholes in the Au layer undetectable by AFM or points of disadhesion probed by the ≈1-mm^2 spot size of the XPS. The AFM image of Au/D/Si (Figure 2b) exhibits no large features, and the surface topography is clearly considerably less rough overall. Note also that XPS analysis of the Au/D/Si sample is consistent with a completely continuous Au layer. Quantitative three-parameter roughness analyses of the two AFM images in Figure 2 were carried out using the height-to-height correlation function, $H(r)$.[20] $H(r)$ is defined as $H(r) = \langle [h(r) - h(0)]^2 \rangle$, where $h(r)$ and

(21) Oliver, W. C.; Pharr, G. M. *J. Mater. Res.* **1992**, *7*, 1564−1583.

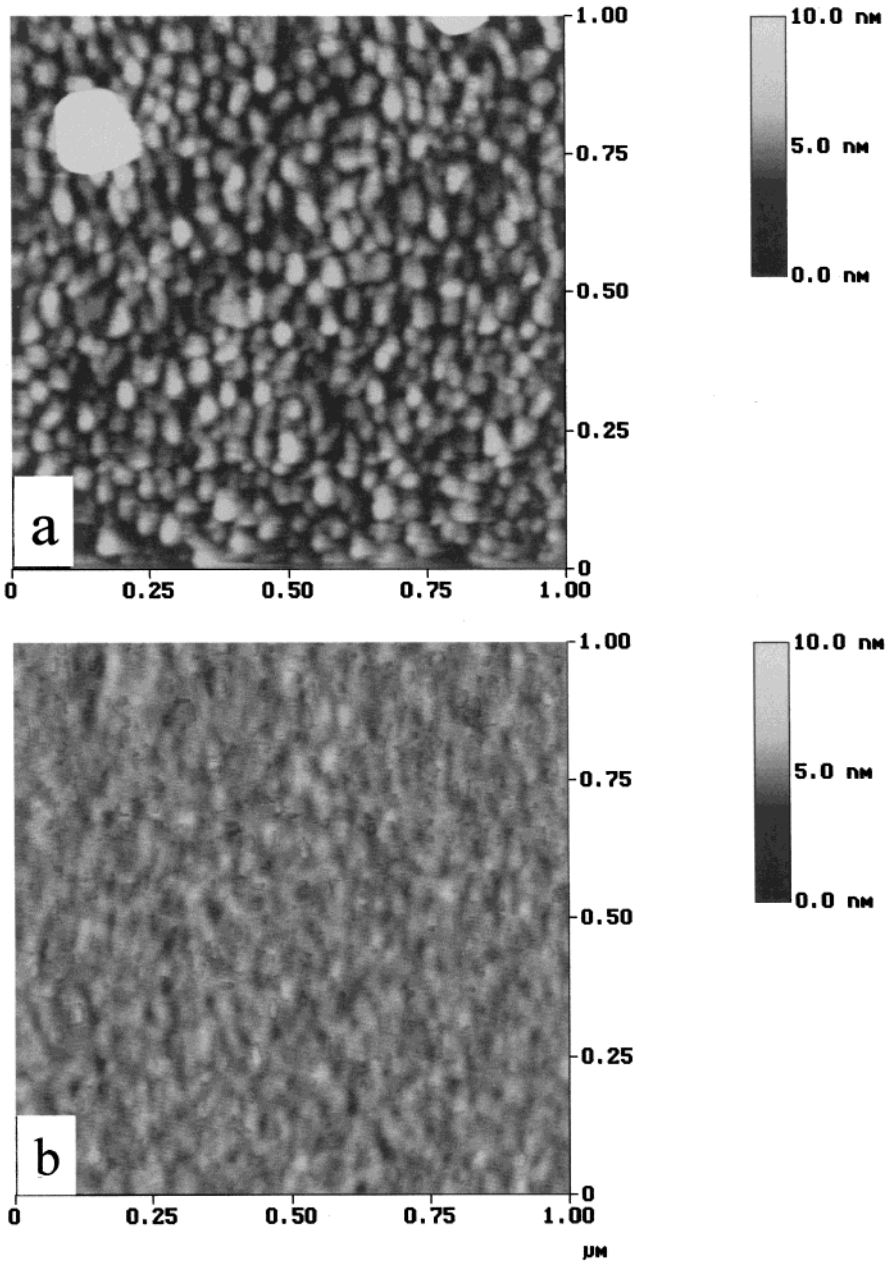

Figure 2. Tapping mode AFM images (1 × 1 μm; 10-nm vertical scale) of samples Au/Si and Au/D/Si.

$h(0)$ are the heights at r [$=(x,y)$] and the reference position (0,0) and the brackets $\langle ... \rangle$ indicate a spatial average. In Figure 2a the large cluster in the upper left corner was excluded from the analysis. In addition to the usual rms vertical roughness (or interface width), w, the correlation (lateral) length, ζ, and the roughness exponent, α, which is indicative of the "jaggedness" of the topography, were extracted from fits to $H(r)$ versus r plots using

$$H(r) = 2w^2[1 - \exp(-r/\zeta)^{2\alpha}] \qquad (2)$$

Representative $H(r)$ versus r plots appear in Figure 3 for both Au/Si and Au/D/Si along with the roughness parameters deduced from fits to the data. The presence of the dendrimer interlayer significantly reduces the vertical rms surface roughness by roughly a factor of 2 from 1.06 to 0.45 nm. Interestingly, the correlation length for the two samples is essentially the same, ≈50 nm. The physical origin of this lateral length scale is not obvious. Since it is unaffected by the absence of the dendrimer layer, we conclude that it is not associated with the center-to-center dendrimer spacing. Another obvious possibility is that the correlation length is controlled by the crystalline grain size in the Au layer. However, grain size estimates based on peak width measurements using XRD (in both symmetric and asymmetric geometries) indicate that the Au grains are 9−10 nm for both Au/Si and Au/D/Si. These approximate grain sizes are in line with expectations based on the Au film thicknesses, although the important point is their similarity and not the actual value. Roughness exponents should fall in the range $0 \leq \alpha \leq 1$ for self-affine fractal surfaces, with a larger value generally indicating a slightly smoother surface in the short range.[22] The Au/D/Si surface is slightly rougher than the native SiO_x of the wafer, which typically has a rms roughness of ≈0.1 nm across a 1-mm line scan.

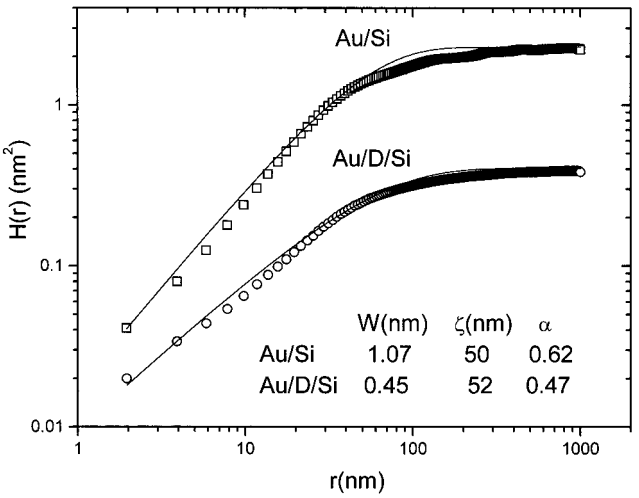

Figure 3. Representative height-to-height correlation function plots, $H(r)$ versus r, derived from the AFM images for Au/Si and Au/D/Si found in Figure 2 along with roughness parameters deduced from fits to the data.

The obvious differences in surface topography between Au/Si and Au/D/Si films as revealed in the AFM images are clearly the result of the different interactions at the respective interfaces. Evaporated Au does not readily wet the native silica surface, at least initially, preferring to self-aggregate, hence, the presence of larger scale features. Ultimately, the Au does wet the surface, forming an essentially continuous layer, but one with relatively poor adhesion to the oxide surface. This is a well-known problem for Au/SiO_x systems and the reason metallic interlayers of Ti or Cr are usually deposited on the SiO_x surface before Au deposition. The presence of a dendrimer monolayer may affect the growth mode of Au either through standard surface energy considerations or by physically limiting the mobility of the deposited Au atoms.

X-ray Reflectivity Measurements. XRR data have been obtained for the samples described in Figure 1. For the G8 dendrimer monolayer alone, the fit of the XRR data indicates the thickness to be 4.6 nm (Figure 4 and Table 1), compared to the spherical diameter of the free molecule in solution of 9.7 nm [Dendritech]. This result is in very good agreement with previous studies of the structure of isolated dendrimers adsorbed on Au as measured by AFM (3.5−4.0 nm)[23] and the trend of XRR results for similar G4 (1.8 nm), G6 (2.8 nm), and G10 PAMAM dendrimers (5.6 nm).[24] Our results are somewhat higher than recent AFM results for a series of PAMAM dendrimers visualized by AFM on mica (G8 observed height ∼2.5 nm).[25] The observed differences may result from differing surface interaction strengths on different surfaces. Several groups have pointed out that AFM measurements of the film thickness of organic monolayers are consistently lower than is indicated by other methods, possibly as a result of physical, tip-induced deformation of the molecules.[23,26,27] In addition,

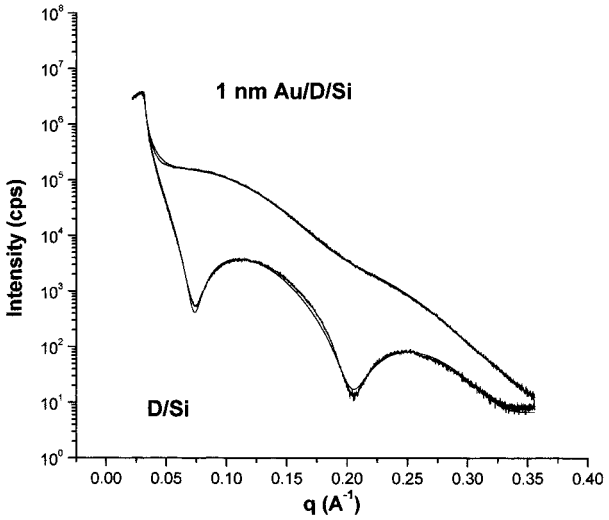

Figure 4. X-ray reflectivity measurements and fits to the data for D/Si and 1-nm Au/D/Si.

Table 1. Tabulated X-ray Reflectivity Data

layer	thickness (nm)	roughness (nm)	density (g/cm³)
D/Si	4.63 ± 0.3	0.64 ± 0.2	1.10 ± 0.2
1-nm Au/D/Si			
mixed layer	1.87 ± 0.2	0.74 ± 0.2	7.64 ± 0.2
dendrimer	3.26 ± 0.2	0.54 ± 0.2	1.44 ± 0.2
12.5-nm Au/D/Si			
Au layer	12.20 ± 0.2	1.08 ± 0.2	19.31 ± 0.2
12.5-nm Au/Si			
Au layer[a]	11.88 ± 0.4	1.65 ± ?	16.3 ± 0.3
SiO_x	2.9 ± 0.3	0.46 ± 0.2	2.41 ± 0.2
Si(100)		0.5 ± 0.2	2.33

[a] This layer does not appear to be homogeneous at examined length scales as a result of disadhesion.

AFM measurements made on isolated dendrimers differ from those on complete monolayers in which lateral intermolecular forces[23] may generate in-plane compressive forces, which could tend to partially offset the natural flattening of adsorbed dendrimers.[24] The compressed or confined nature of the dendrimer monolayer is further confirmed by the XRR measured density of 1.1 g/cm³ in the monolayer compared with 0.81 g/cm³ expected from the molecular weight and free molecule diameter.

XRR data for the Au/D/Si system has also been obtained. For 1-nm Au/D/Si, XRR data clearly show some degree of mixing (Figure 4/Table 1), evidenced by an Au layer density significantly less than that of bulk gold. The XRR data fit indicates that this mixed layer is ≈2-nm thick, with the remaining dendrimer layer at something just >3-nm thick. For the 12.5-nm-thick Au film (Figure 5/Table 1), the fit of the resulting curve is not sensitive to the thickness of the dendrimer layer since the contribution to the reflectivity is overwhelmingly from the Au layer. However, step edge AFM line scans for the 12.5-nm Au/D/Si and Au/Si samples have been obtained.[13] The *overall* thickness of the Au/D is 14.2 ± 0.4 nm by this method, while the thickness of the Au layer alone is 12.5 ± 0.5 nm. These values agree very well with data obtained by XRR and spectroscopic

(22) Chiarello, R.; Panella, V.; Krim, J.; Thompson, C. *Phys. Rev. Lett.* **1991**, *67*, 3408−3411.
(23) Hierlemann, A.; Campbell, J. K.; Baker, L. A.; Crooks, R. M.; Ricco, A. J. *J. Am. Chem. Soc.* **1998**, *120*, 5323−5324.
(24) Tsukruk, V. V.; Rinderspracher, F.; Bliznyuk, V. N. *Langmuir* **1997**, *13*, 2171−2176.
(25) Li, J.; Piehler, L. T.; Qin, D.; Baker, J. R.; Tomalia, D. A.; Meier, D. J. *Langmuir* **2000**, *16*, 5613−5616.
(26) Tsukruk, V. V.; Reneker, D. H. *Polymer* **1995**, *36*, 1791−1808.
(27) Bar, G.; Thomann, Y.; Brandsch, R.; Cantow, H.-J.; Whangbo, M.-H. *Langmuir* **1997**, *13*, 3807−3812.

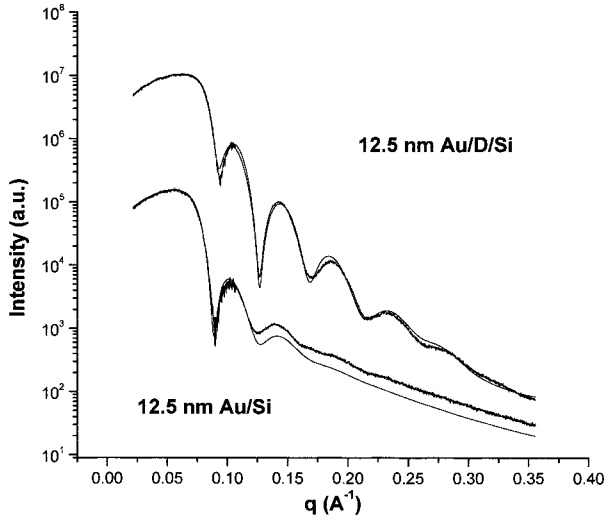

Figure 5. X-ray reflectivity measurements and fits to the data for Au/Si and Au/D/Si as illustrated in Figure 1.

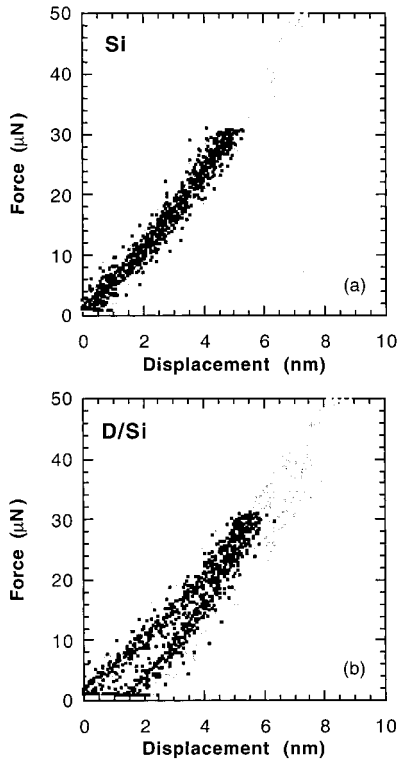

Figure 6. Representative load−displacement curves for maximum loads of 30 (black dots) and 50 μN (gray dots). (a) Si and (b) D/Si.

ellipsometry (not shown). Fits to the XRR data of the Au alone, either as a 1- or 12.5-nm-thick film (Figure 5), are poor since the films are not homogeneous and continuous on the examined length scale. This might be the result of poor Au/Si adhesion, as indicated above.

Nanomechanical Behavior. The nanomechanical responses of the four different sample geometries illustrated in Figure 1 were determined by systematic measurement of load-displacement curves by nanoindentation. In Figure 6 a comparison is made between the force-displacement curves of the Si and D/Si systems. For bare Si (Figure 6a) the observed behavior is almost completely elastic in this very low load regime. The displacements at maximum load (≈5 nm at 30 μN and ≈7 nm at 50 μN) are almost entirely recovered upon release of the load. This behavior is in agreement with recent measurements made by another group using a similar instrument.[28] The load range used here is far below that typically required to generate so-called "pop-in" discontinuities in the load-displacement curves.[28] When identical experiments are performed on the D/Si sample (Figure 6b), it becomes quite apparent that nanoindention is sensitive to the presence of the dendrimer monolayer. The displacements at maximum load increase slightly and clear evidence is found for permanent plastic deformation (a residual or plastic displacement remains after unloading). It is significant that the dendrimers, while certainly softer than the Si substrate, are not simply displaced by the indenter. Substantial elastic recovery of the dendrimer monolayer is apparent.

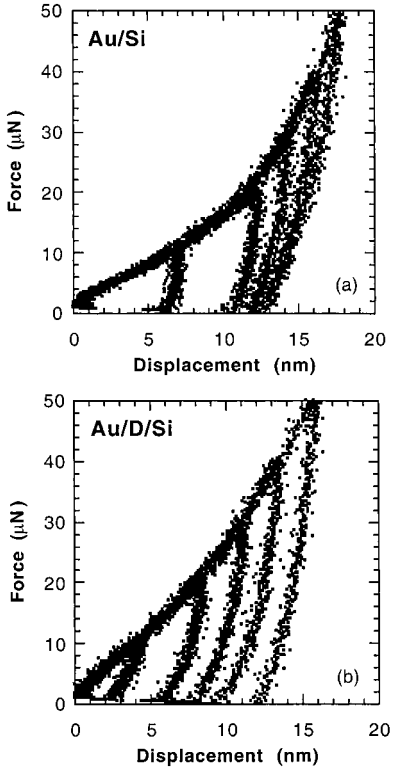

Figure 7. Representative load−displacement curves for maximum loads of 10, 20, 30, 40, and 50 μN. (a) Au/Si and (b) Au/D/Si.

In Figure 7 a comparison is made between the force-displacement curves of the Au/Si and Au/D/Si systems. Pure Au is a very soft metal. This is apparent in Figure 7a where a sequence of force-displacement curves are plotted with systematically increasing maximum force. In contrast to Si, in this load range substantial permanent plastic deformation is observed upon unloading, even using the very smallest maximum load. At least for single-crystal Au surfaces, it is known that unless the probe−sample interaction is passivated by, for example, a self-assembled monolayer of hexadecanethiol, Au will yield plastically upon contact.[15] Note that as the maximum displacement approaches the Au layer thickness, the increment in plastic displacement decreases strongly. In fact, it is very clear that the unloading curves are collapsing onto the displacement

(28) Asif, S. A. S.; Wahl, K. J.; Colton, R. J. *J. Mater. Res.* **2000**, *15*, 546−553.

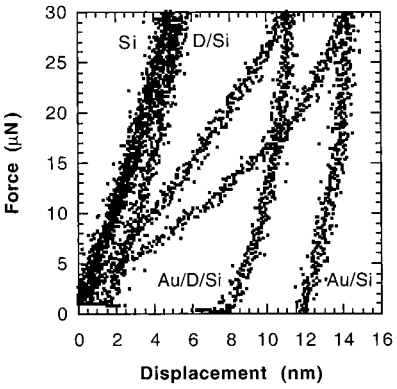

Figure 8. Representative load−displacement curves for all samples at a maximum load of 30 μN.

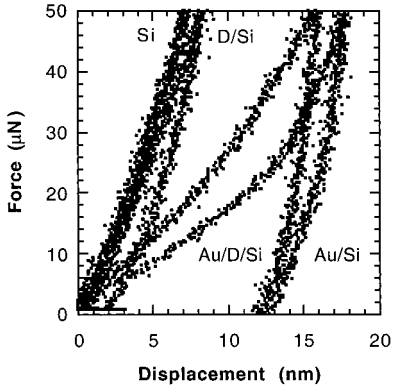

Figure 9. Representative load−displacement curves for all samples at a maximum load of 50 μN.

axis at a position corresponding closely to the measured thickness of the Au film. The interpretation of this observation is that once the indenter tip penetrates the highly plastic Au layer and contacts the Si substrate, further displacements in this loading range are almost fully recovered upon unloading. This behavior persists up to loads as high as 75 μN and corresponding maximum displacements of ≈20 nm, at which point plastic displacement begins to increase again as permanent deformation of the Si substrate begins to come into play. It is apparent that layer thickness can be determined with good accuracy by nanoindention, at least in the special case of a soft layer with small elastic recovery on top of a harder and highly elastic substrate.

If the same force−displacement experiments are carried out on the Au/D/SiO_x sample (Figure 7b), surprisingly large differences are observed, which can only be attributed to the presence of the dendrimer monolayer. The Au/D "bilayer" composite is significantly more resistant to penetration by the indenter tip (maximum displacements at maximum force are lower than those for Au/Si at every load). In addition, the increment in plastic deformation with increasing maximum load is more or less constant; there is no collapse of the unloading curves to a point along the displacement axis. One can only conclude that the Au/D "bilayer" is more resistant to plastic deformation than the same thickness of Au alone.

The nanomechanical responses of the four sample geometries are directly compared for three different maximum loads (30, 50, and 100 μN) in Figures 8−10. Both the 30 and 50 μN loads cause maximum displacements approximately equal to the thickness of the layers studied. At 30 μN (Figure 8) Si is nearly hysteresis-free while D/Si exhibits ≈1.5 nm of permanent displacement. The slope of the initial part of the force−displacement curve is much steeper for Au/D/Si than for Au/Si but the unloading curves are essentially parallel. The improved resistance to plastic deformation afforded by the dendrimer layer is clear. As the maximum load is increased to 50 μN, the Si remains almost purely elastic while D/Si has a slightly increased permanent displacement (Figure 9). The reduced maximum displacement in Au/D/Si versus Au/Si is still clear but the difference between the unloading curves now decreases as the load is released and disappears at complete unloading. The role of the highly elastic substrate becomes increasingly important as loads are increased. The 100 μN load (Figure 10) causes maximum displacements significantly larger than the thickness of the layers studied. At this load some significant permanent deformation of the Si substrate is finally observed. However, the difference between Si and D/Si is still clear. Even for these comparatively large displacements, the smaller maximum displacement in Au/D/Si versus Au/Si remains but the difference between the unloading curves now disappears at finite loads (≈20 μN). The permanent plastic displacement of Au/D/Si is now slightly higher than that of Au/Si.

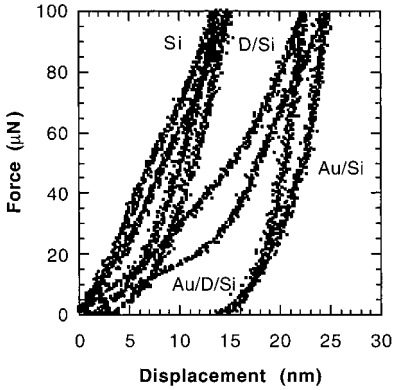

Figure 10. Representative load−displacement curves for all samples at a maximum load of 100 μN.

The nanomechanical behavior of the four samples under consideration can be effectively summarized by comparing percent elastic recovery (%R), maximum displacement, and plastic displacement as a function of maximum load (Figure 11). %R is defined as [1 − (plastic displacment/maximum displacement) × 100]. Consider first %R (Figure 11a). As expected from the load−displacement profiles, Si has the largest %R over the full load range studied. Adsorption of a dendrimer monolayer on Si (D/Si) significantly reduces %R, especially in the low load regime. %R for Si and D/Si converge at high loads as the Si substrate begins to dominate the behavior. The enhanced resistance to deformation afforded by the dendrimer interlayer beneath the Au film (Au/D/Si) is especially clear in the %R plots. Au/D/Si exhibits significantly larger %R than Au/Si at low loads with the difference decreasing with load until it is eliminated by ≈50 mN. At higher loads Au/Si exhibits somewhat higher %R but the two systems converge again at the highest load studied. In the maximum displacement data (Figure 11b) the four

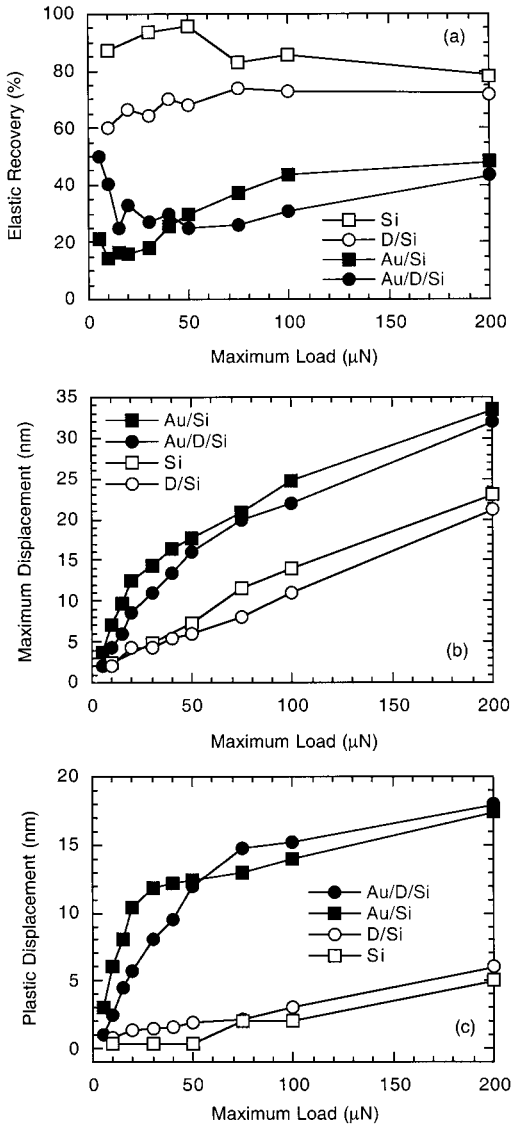

Figure 11. Summary of nanomechanical response versus maximum load for all samples. (a) % elastic recovery, (b) maximum displacement, and (c) plastic displacement.

samples maintain their rank order over the entire load range with D/Si < Si < Au/D/Si < Au/Si. The plastic displacement data (Figure 11c) mirrors the trends found for %*R*. At low loads Si experiences negligible plastic displacement. Addition of the dendrimer monolayer leads to small increases in plastic displacement at low loads. For the pair of Au samples it is again very clear that, below 50 μN, Au/D/Si is significantly more resistant to permanent deformation than Au/Si. The crossover observed at $\approx$50 μN both here and in the %*R* data coincides with the plastic displacement approaching and then exceeding the Au and Au/D thicknesses.

The nanoindentation hardness and modulus of all four samples has been determined as a function of load. We confine our attention to the Au/Si and Au/D/Si samples here. In all cases, the elastic moduli calculated from the load−displacement curves were found, not surprisingly, to be dominated by the response of the Si. Only small deviations from a mean value of $\approx$140 GPa measured for the Si sample were noted. By contrast, for the case of a soft film on a harder and highly elastic substrate, it is quite possible to obtain hardness values indicative of the intrinsic behavior of the soft layer, even for thin layers where displacements approach the film thickness. This is the case for Au/Si and Au/D/Si. For Au/Si, in the low load regime, where the permanent deformation is confined to the Au layer, a nanoindentation hardness of 1.8 GPa is found. This is in good agreement with nanoindentation hardness values reported for single-crystal Au samples.[17] For Au/D/Si a consistent value of 3.2 GPA is observed in the low load range. This hardness enhancement due to the dendrimer monolayer is very intriguing and without obvious explanation. If the grain size in the Au layer were significantly modified by the presence of the dendrimer monolayer, it would be reasonable to suppose that the hardness enhancement might be due to a Hall−Petch-type behavior in which the hardness is proportional to (grain size)$^{-1/2}$ (e.g., ref 29). However this cannot be the explanation here as the mean XRD determined Au crystallite size in the Au/D/Si samples was $\approx$10 nm versus $\approx$8.5 nm in Au/Si. Both grain size numbers are of the same order as the Au film thickness, indicating that on average the Au layer is composed of a single layer of grains. The most reasonable, if tentative, explanation for the observed behavior lies in the nature of the dendrimer monolayer itself, the effect of Au on the monolayer, and the properties of the hybrid nanocomposite created in a limited thickness region where the dendrimers and evaporated Au mix. Strong arguments have been advanced that dendrimer molecules in a monolayer are highly compressed both normal to the substrate and laterally within the monolayer.[24] The effect of such confinement on mechanical response is not easy to predict but it is clear that such a densified structure should be stiffer and more resistant to deformation than one might expect on the basis of the density and structure of the free dendrimer molecules in solution. In fact, very recently a surface force balance apparatus has been used to study the mechanical response of generation 5 poly(propylene imine) monolayers under compression normal to the monolayer.[7] This work clearly demonstrates a rapid increase in modulus with compression after a soft initial response. This observation is accounted for in terms of relatively easy deformation associated with collapsing the less dense core at low loads followed by strong resistance to further deformation due to the solidlike character of the dendrimer shell. It is not unreasonable to imagine that the Au film deposited on top of the dendrimer monolayer in our experiments may further confine the monolayer, leading to a solidlike, incompressible dendrimer layer with a density corresponding to that of the dendrimer outer shell, which is highly resistant to deformation. Interpenetration of evaporated Au into the dendrimer monolayer could also play a role in minimizing dendrimer free volume and contribute to the observed mechanical strengthening. New studies are underway using different dendrimer monolayers and overcoats to further explore the potential of organic/inorganic nanocomposites as tribomaterials.

Conclusions

Several conclusions have been reached, on the basis of AFM, XRR, and XPS studies, about the growth and

(29) Weertman, J. R. *Mater. Sci. Eng. A* **1993**, *166*, 161−167.

chemical interactions of the component layers illustrated in Figure 1. Ultrathin (12.5 nm) Au grown on the native oxide of Si(100) results in an apparently continuous but poorly adherent film with vertical rms roughness ≈1 nm and occasional very much larger scale (≈75 nm) features. Dendrimer-mediated Au films have substantially reduced roughness (≈0.4 nm) and no large-scale features. Detailed roughness analysis does not show significant lateral correlation length differences between the two Au films, indicating that the dendrimer interlayer does not impact the in-plane topography of the metal film. XRR and AFM line scan measurements agree on the film thicknesses and vertical roughness parameters. Conventional XRD indicates that the grain size in both films is slightly less than the Au layer thickness. XPS and XRR of thinner Au films clearly show some degree of mixing between the metal and the dendrimer layer. A comparison of the Au films on Si(100) with and without the dendrimer interlayer shows significant differences in the morphology of the films, particularly vertical roughness, but there is no evidence for distinct microstructural differences in the crystalline Au films (e.g., grain size). Nevertheless, nanoindentation studies demonstrate large differences in the mechanical responses of the two films. The nanoindentation hardness of the dendrimer-mediated 12.5-nm Au film is surprisingly high, higher than the 12.5-nm Au layer alone. This mechanical strengthening is tentatively attributed to the compressed nature of the dendrimer interlayer.

Acknowledgment. This work is supported by the MRSEC program of the NSF under Award DMR-9809423. We would like to thank Prof. Greg Szulczewski for the initial Au depositions.

CM000981E